TYPHOON KARDING (NORU) STORM SURGE ANALYSIS USING THE COAWST MODELING SYSTEM

L. I. J. Nioko[1*], K. M. C. Tablang[1], A. M. Tamondong[1], M. R. C. O. Ang[1], D. M. Bautista[2]

[1] Department of Geodetic Engineering, University of the Philippines Diliman, Quezon City, Philippines
– (ljnioko, kctablang, amtamondong, moang)@up.edu.ph
[2] Institute of Civil Engineering, University of the Philippines, Diliman, Quezon City, Philippines – dmbautista2@up.edu.ph

KEY WORDS: typhoon, storm surge, ocean modeling, COAWST, model coupling

ABSTRACT:

The Philippines, frequently affected by typhoons, faces the hazard of storm surges. This study examined the Coupled-Ocean-Atmosphere-Wave-Sediment Transport Modeling System (COAWST) to simulate Typhoon Karding's September 2022 storm surge. COAWST integrates the Regional Ocean Modeling System (ROMS), Simulating WAves Nearshore (SWAN), and Weather Research and Forecasting (WRF) coupled using the Model Coupling Toolkit (MCT). Four setups were analyzed: i. ROMS only, ii. ROMS-SWAN, iii. ROMS-WRF, and iv. ROMS-SWAN-WRF, focusing on four variables: a. Surface air pressure, b. Wind speed, c. Free-surface elevation, and d. Significant wave height.

Results show that the ROMS-WRF and ROMS-SWAN-WRF setups accurately simulated Typhoon Karding's track with minimal positional error and wind speed. However, the models overestimated the typhoon's minimum air pressure with p-biases of 7.74% (i and ii), 4.1% (iii), and 3.9% (iv), and RMSE values of 68.529 hPa (i and ii), 36.744 hPa (iii), and 36.789 hPa (iv). Additionally, water levels were underestimated, with RMSE ranging from 0.31 to 0.35 meters and p-biases from -72.56% to -154.89% at Baler, Aurora validation point. At the Real, Quezon validation point, RMSE and p-bias ranged from 0.30 to 0.34 meters and -84.80% to -166.44%, respectively. Nonetheless, the models were able to simulate the storm surge and significant wave height at Baler and Real points similar to recorded data, with setup iv performing best in storm surge simulation. In summary, COAWST may be employed for typhoon simulations, with coupling being able to increase accuracy.

1. INTRODUCTION

1.1 Background

The Philippines is one of the most typhoon impacted countries in the world. On average, 20 tropical cyclones (TCs) enter the Philippine Area of Responsibility (PAR) region per year–the most in the entire world. In 2019, on their Annual Report on Tropical Cyclones (ARTC), PAGASA reports that 21 TCs occurred in the country that caused, both directly and indirectly, and despite the country's best efforts in disaster risk reduction and management, the deaths of 67 individuals, 691 injuries, 19 missing persons report, and Php 11.270 billion in damages.

Present studies regarding storm surge modeling treat and investigate variables such as the ocean, waves and tides, atmosphere, and other geomorphological processes independently, where in reality, they occur and affect each other all at the same time. Model coupling is used for communication and interchange of information between these individual models, which may lead to better results. One such system which provides model coupling is the COAWST modeling framework developed by the United States Geological Survey (USGS) for studies involving typhoons, their characteristics, and impacts, and interactions with our coastlines.

1.2 Statement of the Problem

COAWST has been used in studying various earth phenomena and processes, such as ocean-atmosphere dynamics and interactions, modeling of water masses and variability of ocean circulation (Mendonça, et al., 2016), among others. The developers of COAWST, also used it in 2014 to hindcast Hurricane Ivan which hit the United States in 2004.

In the Philippines, typhoon-related phenomena, especially storm surge, are rarely modeled. Nakamura, et al. (2015) provides an evaluation of the storm surge caused by one of the more prominent typhoons to hit the Philippines in Yolanda, using WRF, SWAN models, and the Finite Volume Community Ocean Model (FVCOM) as the ocean component instead of ROMS which is used in COAWST.

Another software suite dealing with water phenomena, Delft3D has been used in the Philippines by Rivera and Hernandez (2018) in building hydrodynamic models DelfT-FLOW, in assessing the flooding problem around Laguna de Bay. Furthermore, Suarez et al. (2015) also utilized Delft3D in building hydrodynamic models in the coastal regions in the Visayan islands for the storm surge simulation of Typhoon Yolanda, resulting in a storm surge inundation map.

COAWST's availability as an open-source program, as well as the existence of its coupling options, provide a free counterpart to proprietary modeling software which are commonly used in storm surge modeling.

1.3 Rationale

Given this, the researchers used COAWST in the analysis of the storm surge caused by Typhoon Karding in September 2022 to assess the applicability of the coupled models in the Philippine setting. In building the models using COAWST, the researchers integrated an ocean model (ROMS), a wave model (SWAN), and an atmospheric model (WRF).

* Corresponding author

1.4 Scope and Limitations

This research focused on a small domain in the Philippines, specifically in the areas hit by Typhoon Karding on September 24, 2022 18:00 UTC+00:00 to September 27, 2022 00:00 UTC+00:00.

The grid domains used in this study, as shown in Figure 1, covers Polillo Island, Jomalig Island, Real and Baler Aurora, and Infanta, Quezon, areas that were directly affected by Typhoon Karding on its first landfall in the country.

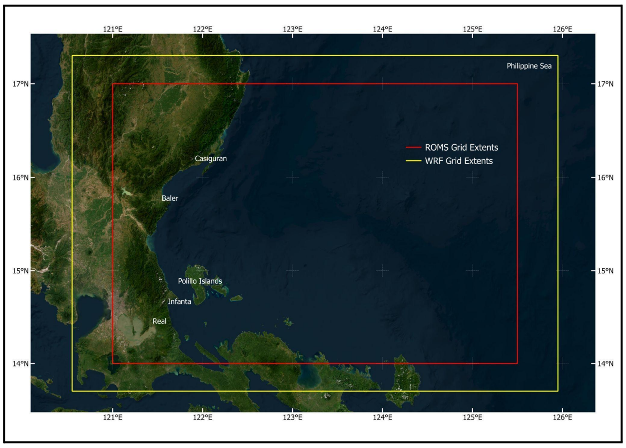

Figure 1. Map showing ROMS and SWAN (red) and WRF (yellow) grid locations.

Furthermore, this research focused on the simulation, computation, and analysis of the induced storm surge of Typhoon Karding relative to the subject area, and exclusively utilized the COAWST modeling framework in all pertinent model building and analysis. Lastly, the researchers used ROMS as the ocean model, WRF as the atmosphere model, and SWAN as the wave model.

In addition, model calibration was not conducted mostly due to insufficient data and time constraints. Only the default coupling options provided by the framework were used and results were taken as is to compare with the validation data. For tidal validation, hourly tidal in situ observational data at two stations only (Real, Quezon and Baler, Aurora), and the only the best-track data from Japan Meteorological Agency (JMA) and Joint Typhoon Warning Center (JTWC) were used for the atmosphere validation.

2. REVIEW OF RELATED LITERATURE

2.1 Ocean modeling

With the advent of computers, wide range of tasks such as mathematical computations are able to be automated and expedited, and alongside the increase in efficiency for computing power as technological advancements occur, models became easier to build and develop, with uses involving mathematical models and analysis of scientific phenomena and processes that occur in the world. In modeling earth systems, various components are typically involved, including but not limited to climate, hydrological processes, weather, atmosphere, and geodynamics (Department of Energy, n.d.).

While independent models can be used to simulate natural phenomena, complex interactions occur between different components of the earth systems. With model coupling, communication and interchange of information between these models are possible, which may lead to better results. (Helmholtz-Zentrum Hereon, n.d.).

2.2 COAWST Overview

COAWST (A Coupled Ocean-Atmosphere-Wave-Sediment Transport) is a modeling framework initially developed and further improved by the USGS. The approach was first developed by Warner et al. (2010). It integrates several components: ocean, wave, atmosphere, and sediment transport models, and a coupler for coupling these models. This study uses the usually used Regional Ocean Modeling System (ROMS) for ocean, Simulating WAves Nearshore (SWAN) for waves, and Weather Research and Forecasting (WRF) for atmosphere, which are coupled by the Model Coupling Toolkit (MCT) and whose fields which can be integrated are shown in Figure 2.

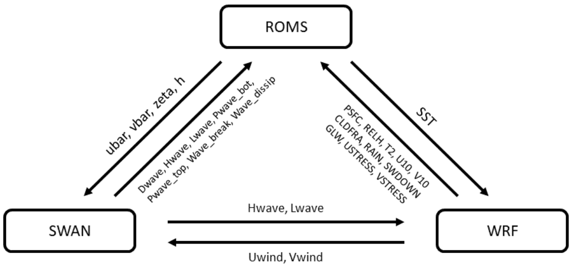

Figure 2. Data fields exchanged between each component.

In Asia, Mo et al. (2021) used COAWST to develop a numerical model and use it to examine the interaction between surface gravity waves and ocean currents during cold air outbreaks in the northern East China Sea in 2014 and 2015, revealing that revealed that wave–current interactions improved the simulation accuracy. Lim Kam Sian et al. (2020) provides an examination on the effects of model coupling using COAWST in the simulation of 2014 Typhoon Kalmaegi which passed across the Philippines on its track. The study highlights the importance of atmosphere–ocean feedback for accurate simulations, such as in a fully-coupled model, while noting to "mind the computational cost of running a fully coupled model, the increased complexity of the numerical equations, model biases and dynamical errors".

While COAWST has seen extensive usage globally and in numerous disciplines, the uncommonness of usage of COAWST, specifically in the Philippine setting and especially for storm surge which is a big hazard especially in the coastlines east of the Pacific Ocean, makes this study compelling to be undertaken.

3. METHODOLOGY

3.1 Study Area and Time Period

The researchers applied COAWST in order to investigate Typhoon Karding (international name Noru) and its induced storm surge. Typhoon Karding originated far east of the Philippines on September 21, 2022, and was designated as a Tropical Depression on September 22, 2022. The study investigated Typhoon Karding from its rapid intensification and PAGASA's promotion of it to super typhoon east of Infanta,

https://doi.org/10.5194/isprs-archives-XLVIII-4-W8-2023-403-2024

Quezon on September 24, 2022 18:00 UTC+00:00, a few hours until its landfall at Polillo Islands and Dingalan, until September 27, 2022 00:00 UTC+00:00.

3.2 Model Setup

Four COAWST system configurations were investigated in this study. Ocean, wave, and atmosphere components in the Regional Ocean Modeling System (ROMS), Simulating WAves Nearshore (SWAN), and Weather Research and Forecasting (WRF) respectively are used, which are most relevant to typhoon analysis. They are summarized in Table 1. In addition to the four configurations, an additional baseline model without the typhoon conditions was run to provide comparison on regular water levels in the studied locations.

Setup name	Ocean model / typhoon forcing	Wave model / wind forcing	Atmospheric model
R	ROMS / ERA5	None	None
RS	ROMS / ERA5	SWAN / ERA5	None
RW	ROMS / WRF	None	WRF
RSW	ROMS / WRF	SWAN / WRF	WRF

Table 1. Summary of model setup.

3.3 Grid description

The computational domains of the ROMS grid and WRF grid, relative with Philippine coastline boundaries, are as plotted in Figure 1. Relevant information about each model's grid is displayed in Table 2. The SWAN grid used in this study is converted from the ROMS grid, thus they share the same properties.

Properties	ROMS / SWAN	WRF
Extents	14 N to 17 N 121 E to 125.5 E	15.5 N ± 600 km 123.25 E ± 400 km
Resolution	1/60°	5 x 5 km grid size

Table 2. Grid descriptions.

3.4 Materials

The bathymetry of the ROMS computational grid was extracted from *GEBCO 2022*. For the ocean component (ROMS), the tidal forcing used is *TPXO9-atlas*, the initial and boundary conditions are obtained from *HYCOM GOFS 3.1*, and the surface forcing is obtained from *ERA5 hourly data on single levels from 1940 to present*.

Moreover, the boundary conditions (wave data) and the wind data for SWAN is obtained from *ERA5 hourly data on single levels from 1940 to present* as well. For WRF, the input files were prepared using the *WRF Pre-Processing System*, with *WPS Static Geography Data* as geographical input, and the *NCEP GDAS/FNL 0.25 Degree Global Tropospheric Analyses and Forecast Grids* as atmospheric forcing.

For observational data to be used for comparison to the model results, *Hourly tidal observations for September 2022, in Real, Quezon and Baler, Aurora stations,* from Philippines' National Mapping and Resource Information Authority (NAMRIA) were used as in situ tidal data, while Japan Meteorological Agency (JMA) and Joint Typhoon Warning Center's (JTWC) *Best Track Data* on Typhoon Noru were used for weather observational data.

3.5 Variables Investigated and Validation

The relevant variables investigated in this study are Surface air pressure (Pair), Surface u,v wind component (Uwind and Vwind), Free-surface height (zeta) - water level, and Wind-induced Significant Wave Height (Hwave), which are then compared to the observational data from JMA and JTWC best track data on Typhoon Karding, as well as tide station data obtained from NAMRIA in Baler, Aurora and Real Quezon.

The minimum surface air pressure was investigated for the tracking of Typhoon Karding, while the rest of the variables were used for the analysis of the storm surge. All relevant variables were extracted and processed from the output NetCDF history file using Climate Data Operator (CDO).

For the positional tracking of Typhoon Karding, the x/y indexes and latitude and longitude of the cell with the minimum surface air pressure per timestep were obtained. The positions of each model were compared to the JTWC and JMA best tracks for validation. Position errors at the times of comparison were found by computing for the Euclidean distance between the model's position and the validation. For the similarity measurement, the mean of the position errors were computed.

$$\text{position error} = \text{sqrt}[\ (x_2 - x_1)^2 + (y_2 - y_1)^2\ ] \quad (1)$$

From the U and V wind components, the wind speeds are computed using the equation:

$$WS = \text{sqrt}(\ U^2 + V^2\ ) \quad (2)$$

Following Japan Meteorological Agency's (JMA) definition of the maximum sustained wind, the 10-minute average (every two timestep) was computed for the maximum sustained surface wind speed in knots.

Water level values were obtained from the ROMS free-surface height (zeta) variable, which is referred to the Mean Sea Level (MSL) through the GEBCO bathymetry used. The water level and significant wave height values for the Baler and Real validation points were extracted using CDO at 15.773 N, 121.636 E and 14.652 N, 121.619 E for the two stations, respectively, which are the closest coordinates without land masking to the provided station coordinates by NAMRIA, which are listed in Table 3 and shown in Figure 3.

Station	Latitude	Longitude
Baler	15° 45' 25.94" N	121° 35' 20.66" E
Real	14°40' 16.48" N	121° 36' 48.43"E

Table 3. Tide station coordinates provided by NAMRIA.

Simulations were run on running COAWST 3.7 under Ubuntu 20.04 via Windows Subsystem for Linux. The ROMS-only and ROMS-SWAN setups took around 3 hours to finish, while ROMS-WRF and ROMS-SWAN-WRF took around 4 to 5 hours. The time needed to complete the simulations increases as the number of coupled components increases.

Thus, the 3-way coupled setup took the longest time to complete given the additional required processing power. It is important to note that the computational grid used is relatively coarse and the time period is short, but sufficient enough for general typhoon simulation. It is expected that for finer resolutions, i.e., in closer coastal analysis, computational time will increase.

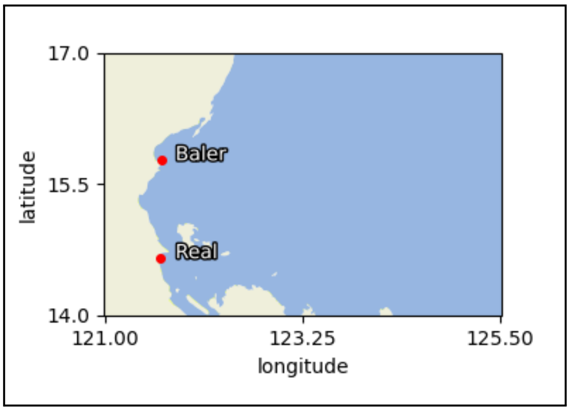

Figure 3. Map showing the tide station coordinates in the ROMS grid.

Following Mo et al., 2021, variable outputs from each setup are evaluated by comparing the simulated data with in situ observations using two statistical measures: (a) root-mean-square error (RMSE), and (b) correlation coefficient R^2. The RMSE is computed by comparing the time series of the simulated and observed data; the correlation coefficient is calculated for the time series of the simulated and observed data (Mo et al., 2021). Additionally, following Mamnun et al., 2020, the percentage model bias (p-bias) for each model variable was also calculated. The p-bias gives a quantitative measure of how the model is under or over predicting the observed data.

The air pressure, typhoon track from the pressure, and the wind speed simulated from the models were compared with the best-track data from Japan Meteorological Agency (JMA) and Joint Typhoon Warning Center (JTWC). Due to lack of availability of the best-track data of pressure, position, and wind speed from PAGASA at the time of writing, PAGASA preliminary data are not considered in this analysis. Moreover, for the said variables, only four time periods from JMA Best Track and from JWTC (6-hour interval)—Sept. 24 18:00:00, Sept. 25 00:00:00, Sept. 25 06:00:00, Sept. 25 12:00:00—are used as Karding is already outside of the computational grid after Sept. 25 12:00:00.

Hourly in situ tidal observations for September 2022, in Real, Quezon and Baler, Aurora stations obtained from NAMRIA were used to validate the water level data computed from the models. A ROMS model forced with tides and normal atmospheric conditions was simulated to serve as a baseline model. The generated surge was computed by getting the difference (residual) between the free-surface height of the typhoon models and the baseline model.

For the significant wave height, the models with SWAN are investigated and compared with the forecast advisories, due to the lack of observational data with regards to waves. Both free-surface height and significant wave height are compared a few hours after the start of the simulation at September 25, 00:00 UTC+00:00, for the fields to stabilize, until September 27 00:00 UTC+00:00, to check how the water level compares even after the typhoon has passed already.

4. RESULTS AND DISCUSSION

In this chapter, results obtained for the studied variables are presented and analyzed. All time observations are presented in UTC+00:00.

For the analysis of surface air pressure and surface wind, the R and RS setups are treated as one since the simulated results of the setups are equivalent. This is attributed to the lack of the atmospheric model WRF, as without WRF, the models are driven by the same forcing provided by ERA5, yielding the same air pressure and wind speed outputs. Moreover, simulation data after Sept. 25 18:00 were disregarded due to being unrealistic since Karding already approached the masked area of the computational grid after the said time interval.

4.1 Surface Air Pressure and Typhoon Track

The minimum surface air pressure from the model outputs in contrast with the 6-hour interval verification data from JMA and JTWC are compared in Figure 4. The minimum surface air pressure of Karding is reported to be 940 hPa by JMA and 919 hPa by JTWC, observed at the time interval Sept. 25 00:00 UTC. The simulated minimum surface air pressure of the RSW setup is 953.879 hPa, 953 hPa for RW, and 991 .012 hPa for ROMS/RS setup; the RSW and RW setups simulated the minimum air pressure at the interval Sept. 24 22:00, while the ROMS/RS setup simulated the minimum pressure at Sept. 25 08:00 interval.

The computed statistical measures contrasting the simulated surface air pressure values and verification data from JMA and JTWC are shown in Tables 4 and 5, respectively. The minimum surface air pressure of Karding was overestimated by the four studied models, as displayed in Figure 4 and as evidenced by the p-bias % measures shown in Tables 4 and 5. The simulated minimum air pressure values of RSW and RW setups more closely resemble the reported air pressure values by JMA than the observed values by JTWC, as suggested by the RMSE measures. This is mainly due to the significantly higher reported minimum air pressure values reported by JMA as compared to the air pressure data from JTWC, thus resulting in the overestimation bias of the models being lower in the JMA comparisons than the JTWC. Ultimately, the overestimation bias of the models can be attributed to the high values found in the forcing themselves, due to reanalysis data in ERA5 and NCEP's GFS being interpolated from local sensors and sources to form global models.

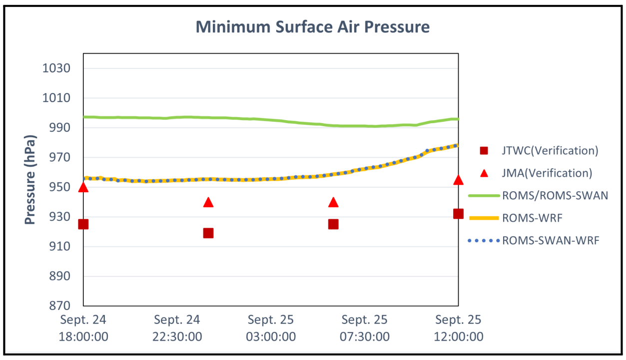

Figure 4. Minimum surface air pressure.

	R^2	RMSE (hPa)	p-bias (%)
RSW	0.4799	16.856	1.60
RW	0.4777	16.798	1.72
R/RS	0.2172	47.628	5.20

Table 4. R^2, RMSE, and p-bias values for the simulated surface air pressure from the four model setups in comparison with the JMA best track data.

	R^2	RMSE (hPa)	p-bias (%)
RSW	0.4799	16.856	1.60
RW	0.4777	16.798	1.72
R/RS	0.2172	47.628	5.20

Table 5. R^2, RMSE, and p-bias values for the simulated surface air pressure from the four model setups in comparison with the JTWC best track data.

The RSW and RW both simulated Karding's landfall at Burdeos, Quezon at the time interval Sept. 25 10:00. PAGASA reports the landfall at time Sept. 25 09:30. The time lag in the simulation of the minimum surface air pressure and the landfall can be attributed to the typhoon movement dynamics driven by the WRF model. The same time lag was also observed in Mamnun et al., 2020.

The position errors are shown in Figures 5 and 6, computed by solving for the displacement difference between the 6-hour interval best-track Typhoon Karding positions by JMA (Figure 5) and JTWC (Figure 6) and the minimum surface air pressure location simulated by the models. The RSW and RW setups resulted in the same typhoon positions, and the ROMS and RS setups yielded the same typhoon positions at the relevant time intervals as well. This can be explained by the relatively coarse computational grid and the methodology used in extracting the locations of the cells with the minimum air pressure.

The average position errors of the models with WRF are 24.88 kilometers and 24.49 kilometers compared with JMA and JTWC verification tracks, respectively. In contrast, the average position errors of the ROMS and RS setups are 17.77 kilometers and 23.58 kilometers compared with JMA and JTWC verification tracks, respectively. However, it is important to note that although the ROMS and RS setups simulated the relatively more accurate typhoon track, the difference between the positional errors of R/RS and RW/RSW is small and could be negligible. Moreover, it is important to note that the R/RS setups overly underestimated the strength of Karding based on its minimum air pressure, while the RW/RSW setups were able to generally capture the minimum air pressure of Typhoon Karding.

The simulated Karding typhoon tracks and the verification from JMA and JTWC best-track data are displayed in Figure 7, showing Karding's track from Sept. 24 18:00 to Sept. 26 00:00 UTC. Throughout the forecast, the RSW and RW simulated tracks are slightly below (southward) than the JMA and JTWC verification tracks. However, the simulated tracks from the four model setups are still able to resolve typhoon Karding's track in comparison with JMA and JTWC best-track data, as evidenced as well by the measured position errors presented in Figures 5 and 6 with position errors ranging from 10 to 45 kilometers. In contrast, Zambon et al. (2014) reported position errors ranging from 20 kilometers to 40 kilometers on their investigation of Hurricane Ivan (2004) for the ROMS-WRF and ROMS-SWAN-WRF setups.

Based on the computed positional errors, the simulated typhoon tracks from the model setups with and without WRF are generally acceptable. In comparison, from PAGASA's 2021 Annual Report, the average forecast-track error from PAGASA forecasts during the fiscal year 2021 is about 45.6 kilometers.

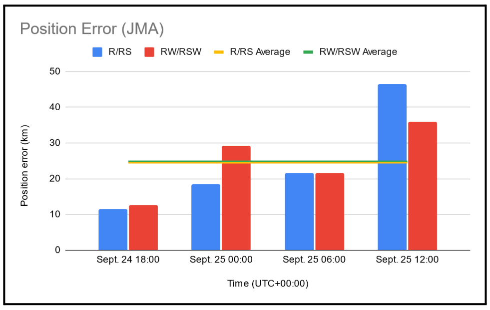

Figure 5. Position error comparing the simulated tracks with JMA best-track data in kilometers.

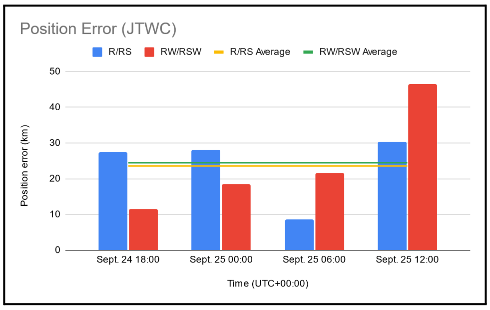

Figure 6. Position error comparing the simulated tracks with JTWC best-track data in kilometers.

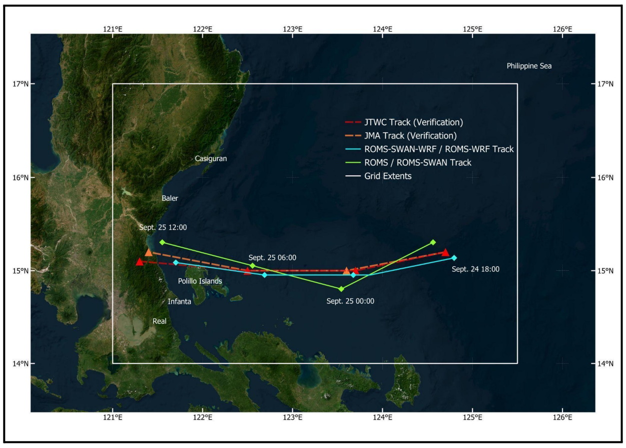

Figure 7. Karding Tropical Cyclone Tracks.

4.2 Surface Wind Speed

Table 6 shows the maximum sustained wind speed in knots of Typhoon Karding at four different time periods, obtained from JMA and JTWC best-track data.

Time	JMA (kts)	JTWC (kts)
Sept. 24 18:00	95	140
Sept. 25 00:00	95	130
Sept. 25 06:00	85	115
Sept. 25 12:00	75	90

Table 6. Maximum sustained wind speed from JMA and JTWC

The significant discrepancy in the wind speed values between JMA and JTWC is attributed to the difference in the maximum sustained wind definition of the agencies: JMA computes for the 10-minute mean, while JTWC computes for the 1-minute mean. For this analysis, maximum sustained wind speed values from JMA are considered, and therefore the surface wind speeds extracted from the model outputs also follow the JMA methodology.

The simulated maximum wind speeds (in knots) computed from the three model setups, with the best-track verification data from JMA are shown in Figure 8. Same with the air pressure, wind speeds from R/RS setups are the same due to being forced by the ERA5 forcing. The computed maximum wind speed from the 3-Way coupled setup and the RW setup closely simulate the best-track maximum sustained wind data from JMA, as evidenced by the R^2 (98% for both) values computed for both setups, shown in Table 7. The same is also suggested by the computed RMSE values of approximately 4 kts for the two setups, as the minimal value of the RMSE for the two setups implies the proximity of the simulated wind speed values and the best-track verification data from JMA. Meanwhile, the minimal negative p-bias computed for the two setups suggest that the maximum wind speeds were slightly underestimated by the models. The highest maximum sustained wind reported in the JMA best-track (95 kts) data is consistent with the simulated wind of both RSW and RW model setups (~96 kts).

In contrast, the setups without WRF, the R and RS setups, were not able to simulate the wind of Karding based on the measures computed, due to the ERA5 wind fields used as surface forcing greatly underestimating the winds.

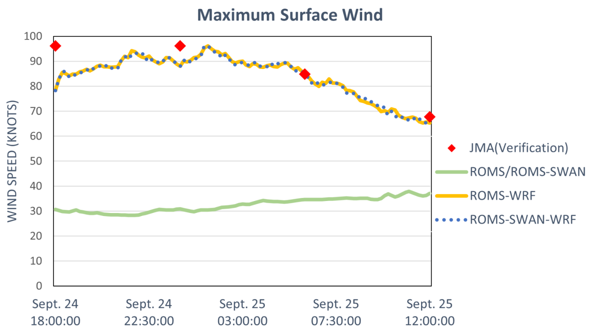

Figure 8. Simulated Maximum Wind Speed: Blue (RSW), Yellow (RW), Lime (R/RS), Red (JMA best-track).

	R^2	RMSE (kts)	p-bias (%)
R/RS	0.5553	53.435	-59.90
RW	0.9691	4.082	-2.10
RSW	0.9724	3.789	-2.30

Table 7.. R^2, RMSE, and p-bias values for wind speed from simulated model setups in comparison with the JMA best track data

4.3 Free-surface height

For the computation of the modeled storm surge, eight total configurations were studied, for the four model setups and two stations in Baler, Aurora and Real, Quezon. Shown in Figures 9 and 10 are the line charts for the results.

For the setups where WRF is coupled, it can be observed that the zeta values at the beginning of the graphs have fluctuating values, attributed to the stabilization of zeta as the fields in the individual models have different values for their respective variables, so it takes a while for the zeta values to balance out. This may be resolved by starting the simulations one or two days earlier.

The R setup was able to generate a minimal surge of around 0.1m, as shown in the top-left chart for both Figures 9 and 10. The RS setup, while being able to generate a surge of up to 0.3 meters as shown in the top-right charts, tends to underestimate the water level starting September 26, when the typhoon has passed the computational grid. RW similarly is able to generate a small surge in both stations, which can be seen in the bottom-left charts. Lastly, the RSW setup (bottom-right) is able to generate a surge in Baler of up to 0.5 m, and around 0.25m in Real.

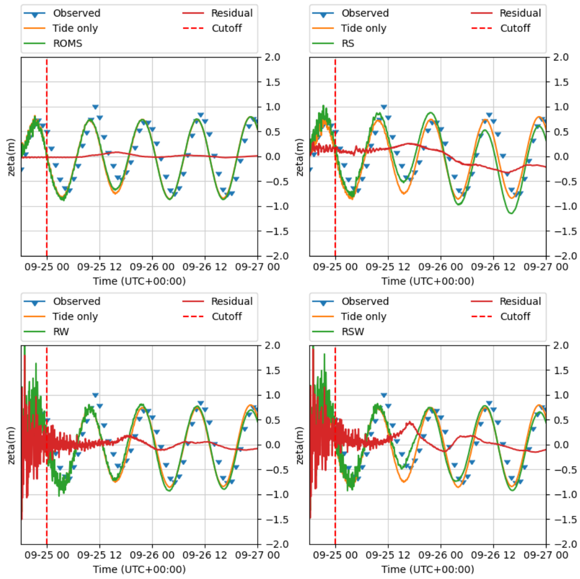

Figure 9. Water levels in the Baler station for the R (top left), RS (top right), RW (bottom left), and RSW (bottom right) setups.

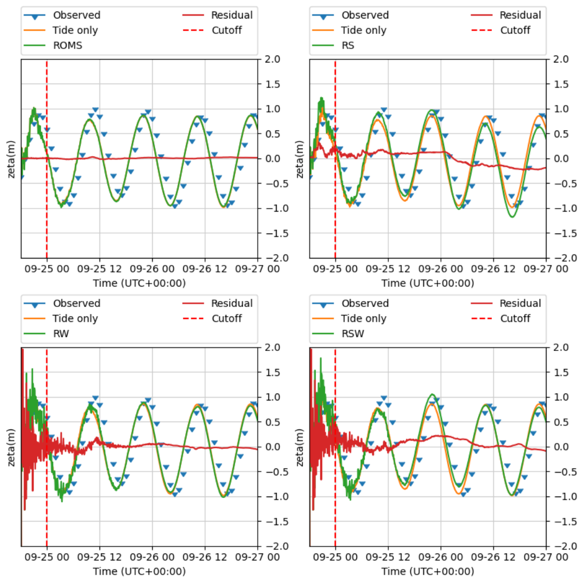

Figure 10. Water levels in the Real station for the R (top left), RS (top right), RW (bottom left), and RSW (bottom right) setups.

For all graphs, the historical observed data from NAMRIA is signified by the inverted blue triangle, the simulated normal tides are in yellow, the simulated storm tides per model are in green, and the residual (difference between simulated normal and storm tide) or the simulated surge is in solid red.

BALER	R^2	RMSE	P-bias (%)
R	0.8703	0.3106	-154.8891
RS	0.8409	0.3521	-130.8648
RW	0.8233	0.3561	-142.4908
RSW	0.8140	0.3341	-72.5591

Table 8. R^2, RMSE, and p-bias values for Baler station

REAL	R^2	RMSE (m)	P-bias (%)
R	0.8804	0.3323	-166.4454
RS	0.8843	0.3403	-141.5882
RW	0.8959	0.3122	-162.5842
RSW	0.8790	0.2962	-84.8048

Table 9. R^2, RMSE, and p-bias values for Real station

Shown in Tables 8 and 9 are the computed R^2, RMSE, and p-bias values for both Baler and Real stations. These were computed from the corresponding times in the model for the available hourly observations of the tide level in the two days of simulation.

All model setups yielded negative P-bias, showing general underestimation of the water levels at the study areas. The R setup has the most positively correlated values from the Pearson's coefficient, and closest RMSE value for both stations. However, it should be noted from the top-left graphs in Figures 9 and 10, the R setup, showing Baler and Real stations' water level respectively, that the modeled surge is severely small and almost negligible, as that the ERA5 forcing underestimated the typhoon intensity.

Out of all setups, RSW has a wider gap in the P-bias than the others, which means that the average values have a tendency to be smaller than observed. The lesser Pearson's r and larger RMSE in the RSW setup may be associated with the fluctuating values at the start. The somewhat randomness in the computed statistical values may be also explained by the limited number of values for comparison due to the hourly nature of the available historical data, which may not be representative of the surge in water levels.

The lower amount of surge in Real may be linked to the weaker ocean currents generated, as Real is obstructed from the wider ocean by Polillo Islands to the east, making them start from Polillo Strait. This also manifests in the shorter propagation time of waves which will be discussed in the next section. Real also being far from the landfall of the typhoon makes it apparent that a high surge is not expected.

4.4 Significant Wave Height

Shown in Figure 11 is the time-series graph of the significant wave height in both Real and Baler stations, for the RS and RSW setups.

In both setups, a rise in significant wave height can be seen for the duration of the passing of Typhoon Noru at the selected sites. For the RS setup however, the rise in Real is almost insignificant, while the rise in Baler has a maximum of about 1 meter height, which can be associated with the underestimation of wind velocity in the ERA5 forcing. In contrast, the RSW setup shows a visible rise in significant wave height for both stations during the passing of the typhoon, the heights reaching up to 4 meters in Baler, and around 1 meter in Real.

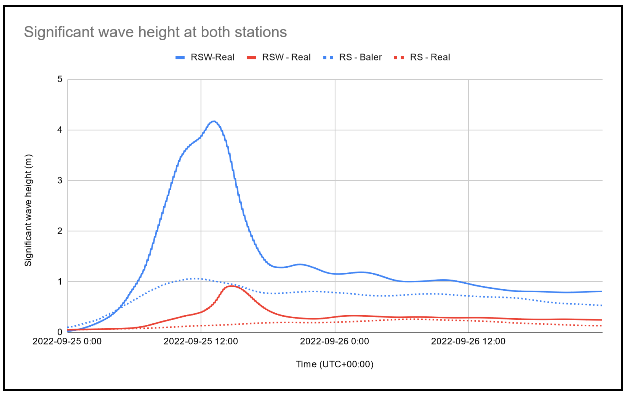

Figure 11. Significant wave height in the RS and RSW setups

The RSW setup is in agreement with the potential storm surge in the PAGASA forecast and advisories archived by Typhoon2000. To quote, "Waves of 2 to 6 meters in height are expected in storm surge-prone areas, particularly in coastal areas where the Tropical Cyclone is headed". This highlights the importance of accurate wind information for the wave model to return corresponding results, which the WRF fields being transferred are able to provide.

5. CONCLUSION

Although slightly overestimated, the RSW and RS setups were able to simulate the minimum surface air pressure brought about by Karding. Similar to the air pressure, the RSW and RS setups were also able to accurately simulate the JMA reported wind speed of Karding. Moreover, the models were also able to simulate the typhoon track of Karding with maximum positional error of approximately 50 kilometers. Lastly, although the models were able to show indications of storm surge from the simulated free-surface and significant wave height, the models without WRF coupling significantly underestimated the relevant values primarily because of the underestimated air pressure and wind values from the ERA5 forcing.

In analyzing the modeled storm surge, the computed statistical measures may not necessarily be the best estimators, due to the low temporal resolution of the historical data, as surges do not always last long or for hours as such the data in between the available points are lacking. Nevertheless, the models show response to typhoon conditions and resulted in a surge in water levels in most setups.

Based on the findings and analysis presented in the previous chapters, the COAWST modeling system may be used to simulate typhoons. Ultimately, this depends on the accuracy of the input, however, a general conclusion may be drawn that given certain weather conditions, in this case a typhoon, COAWST is able to model the resulting development, in this case the impact of a typhoon.

The individual (non-coupled) ROMS, SWAN, and WRF models are applicable for ocean modeling, wave, atmosphere modeling, respectively. So, for simulating the generated storm surge (analysis of water level) of a typhoon, a ROMS only model setup can be used, for analyzing waves (e.g., significant wave height) a SWAN only model setup can be used, and for atmospheric analysis/typhoon tracking, a WRF only model setup can be used. Coupling makes more information available to individual models, most notably for weather or atmospheric modeling, for example, the effect of sea surface temperature to the typhoon simulation provided by the WRF and ROMS coupling.

All model setups investigated in this study are limited in nature such that calibration was not conducted, due to the scarce data availability in the study area as well as limited time and processing power. Moreover, only the default settings provided by the Model Coupling Toolkit included in COAWST were used, not further modifying the interactions between the models. The underestimation and overestimation of model results, while negligible in the bigger scale, might be significant in specific areas. This may be resolved through the calibration of the models to better fine-tune the model response.

In this study, Typhoon Karding and its generated storm surge was modeled, and results show that this is in correspondence to the available observational data. In addition, coupling is helpful in increasing the accuracy of results, especially in the case that reanalysis data which is used in forcing input is not accurate with regards to capturing the typhoon.

6. RECOMMENDATIONS

The researchers recommend the selection of a well-documented typhoon for future studies. This is to ensure the availability of the validation data, particularly of the air pressure, wind, wave, and tidal data. In the local case, since PAGASA only releases their best-track data in their Annual Report on Philippine Tropical Cyclones (ARTC), which are published two years after the end of the typhoon season, it is recommended that future researchers consider this non-availability of best-track data in the typhoon selection. PAGASA also only has land sensor data in select municipalities, which in case available, the time interval available is only every six hours. Moreover, for future studies investigating storm surge in the Philippines, it is recommended that the availability of tidal stations from NAMRIA be checked initially before the selection of the typhoon and the study area.

Furthermore, the researchers recommend further experiments and investigations on the various available model configurations and settings. Additionally, it is recommended for future studies to investigate grid refinement and nesting applications to possibly capture more complex coastal characteristics that could not be resolved with coarser grids. The availability of time and processing and computing power for computers is also advantageous, to be able to run finer-resolution simulations, especially in coastal studies which require more detailed models.

Based on the findings, it is recommended for PAGASA to implement COAWST, given that they already use WRF for weather modeling and forecasting. Doing so would provide insights to the effect of the weather model to the processes occurring in the ocean.

REFERENCES

Department of Energy, n.d. DOE Explains… Earth System and Climate Models. from www.energy.gov/science/doe-explainsearth-system-and-climate-models (20 October 2022).

Helmholtz-Zentrum Hereon, n.d. Atmosphere-Ocean interaction. www.hereon.de/institutes/coastal_systems_analysis_modeling/hydrodynamics_data_assimilation/atmosphere_ocean_interaction/index.php.en (20 October 2022).

Lim Kam Sian, K. T. C., Dong, C., Liu, H., Wu, R., & Zhang, H, 2020. Effects of Model Coupling on Typhoon Kalmaegi (2014) Simulation in the South China Sea. Atmosphere, 11(4), 432. doi.org/10.3390/atmos11040432.

Mamnun, N., Bricheno, L. M., & Rashed-Un-Nabi, M., 2020. Forcing ocean model with atmospheric model outputs to simulate storm surge in the Bangladesh coast. Tropical Cyclone Research and Review, 9(2), 117–134. doi.org/10.1016/j.tcrr.2020.04.002.

Mendonça, L. F., Souza, R. B., Aseff, C. R. C., Pezzi, L. P., Möller, O. O., & Alves, R. C. M, 2017. Regional modeling of the water masses and circulation annual variability at the Southern Brazilian Continental Shelf. In Journal of Geophysical Research: Oceans (Vol. 122, Issue 2, pp. 1232–1253). American Geophysical Union (AGU). doi.org/10.1002/2016jc011780.

Mo, D., Li, J., & Hou, Y., 2021. Assessing the Impact of Wave–Current Interactions on Storm Surges and Waves during Cold Air Outbreaks in the Northern East China Sea. Journal of Marine Science and Engineering, 9(8), 824. doi.org/10.3390/jmse9080824.

Nakamura, R., Takahiro, O., Shibayama, T., Miguel, E., & Takagi, H., 2015. Evaluation of Storm Surge Caused by Typhoon Yolanda (2013) and Using Weather - Storm Surge - Wave - Tide Model. In Procedia Engineering (Vol. 116, pp. 373–380). Elsevier BV. doi.org/10.1016/j.proeng.2015.08.306.

Rivera, P., 2018. MODELING OF STORM SURGE AND FLOOD HAZARD AROUND LAGUNA DE BAY, PHILIPPINES. doi.org/10.31219/osf.io/5zcep.

Suarez, J., May, C., Biton, N. I., Cuadra, C., Joy, S., Jerico, M., & Lagmay, A. M., 2015. Delft3D Storm Surge Simulation of Typhoon Haiyan for Projection of Coastal Inundation in the Visayas Islands, Philippines.

Typhoon2000 Philippine TC Advisories, 2022. Super Typhoon KARDING (NORU) Advisory No. 09. https://typhoon2000.info/karding22_09-2/ (4 June 2023).

Warner, J. C., Armstrong, B., He, R., & Zambon, J. B., 2010. Development of a Coupled Ocean–Atmosphere–Wave–Sediment Transport (COAWST) Modeling System. Ocean Modelling, 35(3), 230–244. doi.org/10.1016/j.ocemod.2010.07.010.

Zambon, J. B., He, R., & Warner, J. C., 2014. Investigation of hurricane Ivan using the coupled ocean–atmosphere–wave–sediment transport (COAWST) model. Ocean Dynamics, 64(11), 1535–1554. doi.org/10.1007/s10236-014-0777-7.